

Optoelectronic property analysis of MCrO_4 (M=Ba, Sr) with a response to visible light irradiation

C.Tablero

*Instituto de Energía Solar, E.T.S.I. de Telecomunicación,
Universidad Politécnica de Madrid,
Ciudad Universitaria s/n, 28040 Madrid, SPAIN.*

e-mail: ctablero@etsit.upm.es

Tlf: +34 915495700

Fax: +34 915446341

Abstract

Ternary MCrO_4 (M=Ba, Sr) semiconductors are materials with a variety of photocatalyst and optoelectronic applications. We present detailed microscopic analyses based on first-principles of the structure, the electronic properties and the optical absorption in which the difference between symmetrically non-equivalent atoms has been considered. The high absorption coefficients of these materials are split into chemical species contributions in accordance with the symmetry. The high optical absorption in these materials is mainly because of the Cr-O inter-species transitions.

Keywords: optoelectronic properties, semiconductors, photovoltaics.

1. Introduction

For solar energy applications there is a need to develop new types of photocatalysts and solar cell materials responding to visible light irradiation. Microscopically, this response is a consequence of the electronic and optical properties. First principles are an important and powerful complementary tool, allowing these basic properties which are hardly accessible by experiments to be obtained and quantified.

MCrO₄ oxides have been of interest as regards their high pressure behavior [1,2] and their photocatalytic properties [3]. In both cases the goal is to explore the possible polymorphs with novel structures and properties that may be used for practical applications.

A number of compounds with the ABO₄ formula and a BO₄ tetrahedral anion polyhedral were found to crystallize in the Hashemite- [4] and Monazite-type [5] structures. In particular, BaCrO₄ crystallizes in the Hashemite structure. This structure shows orthorhombic symmetry with the Pnma space group (n° 62) and lattice parameters (a,b,c)=(9.105,5.541,7.343) Å. On the other hand, SrCrO₄ crystallizes in the Monazite structure with monoclinic symmetry and space group P2₁/n (n° 14), and lattice parameters (a,b,c)=(7.083,7.388,6.771) Å. These structures have usually been described in terms of oxygen polyhedra, the oxide being formed by isolated [BO₄] tetrahedra and complex [AO₁₂] dodecahedra. The Hashemite-BaCrO₄ and monazite-SrCrO₄ crystal structures are shown in Figure 1. Note that in the Hashemite and Monazite structures there are 3 and 4 non-equivalent O atoms, labeled as O_i (i=1,..3 or 4) [4,5] in Figure 1.

The main experimental and theoretical research activities focus on exploring the possible metastable high-pressure structures and structures with photocatalytic properties. However, despite experimental and theoretical research activities, there is little analysis focusing on optoelectronic properties for devices with a response to visible light. With the objective of relating the absorption of the solar radiation with the structure and the microscopic electronic and optical properties we will use first-principles in our analyses.

2. Calculations

In order to obtain the electronic and optical properties we have used first principles based on density-functional theory (DFT) [6] with a private modification of

the SIESTA code [7]. The gap underestimation problems are well known because of the exchange-correlation effect when the standard functionals [7] are used. Therefore, a more profound study is carried out including an orbital-dependent, one-electron potential (DFT+U method) [8-12] to account explicitly for the correlation and to improve the electronic structure description of the states.

The DFT+U results, in addition to the U value, depend on the orbital subspace on which U is applied, and on the orbital occupation numbers [9-12]. In this study we use several U values applied to different orbital subspaces with the GGA+U formalism described in references [9,10]. The generalized gradient approximation from Perdew, Burke and Ernzerhof [13] for the exchange-correlation potential is used. The pseudopotentials adopted are standard Troullier–Martins [14] expressed in the Kleinman–Bylander [15] factorized form. The valence wave functions are expressed with a numerically localized pseudoatomic orbital basis set [16]. Periodic boundary conditions, spin polarization, 120/108 special k points in the irreducible Brillouin zone for Hashemite-BaCrO₄/Monazite-SrCrO₄, and double-zeta with polarization localized basis sets have been used in all the results presented in this work. The electronic structure calculations were carried out by relaxing all the cell atoms using the conjugate gradient algorithm to minimize the calculated quantum mechanical forces. Relaxation to the absolute energy minimum is considered as accomplished when the forces on the atoms fall below 0.004 eV · Å⁻¹.

The optical properties have been obtained from the complex dielectric function

$$e_2(E) \sim \frac{1}{E^2} \sum_{\mu < \lambda} \int d\vec{k} [f_{\mu, \vec{k}} - f_{\lambda, \vec{k}}] |p_{\mu\lambda}|^2 \delta(E_{\lambda, \vec{k}} - E_{\mu, \vec{k}} - E) \quad (1)$$

using the Kramers-Kronig relationships. For the $p_{\mu\lambda}$ matrix elements between the μ and λ bands at \vec{k} points in the Brillouin zone of the momentum operator ($p=i(m/\hbar)[H,r]$),

both the local and non-local parts of the pseudopotentials have been considered. In the previous equation $E_{\mu,\vec{k}}$ and $f_{\mu,\vec{k}}$ are the single-particle energies and occupations of the μ band at \vec{k} points in the Brillouin zone.

3. Results and Discussion.

In the Hashemite and Monazite structures there are 3 and 4 non-equivalent O atoms, labeled as O_i ($i=1,..,n$, with $n=3$ and 4 for the Hashemite and Monazite structures respectively) [4,5] (Figure 1). Considering this non-equivalency the Hashemite and Monazite structures can be represented by $BaCrO_1O_2[O_3]_2$ and $SrCrO_1O_2O_3O_4$ respectively. The non-symmetry-equivalence of the O atoms has been taken into account in all our analyses.

By applying the aforementioned calculation methodology to $BaCrO_4$ and $SrCrO_4$ in the Hashemite and Monazite crystal structures, we have obtained the single-particle band energies. The energy band gaps obtained by taking the difference between the single-particle band energies are 2.70 eV and 2.65 eV with $U=0$ eV for Hashemite- $BaCrO_4$ and Monazite- $SrCrO_4$ respectively, in good agreement with the experimental observation (2.63 for $BaCrO_4$ and 2.44 eV for $SrCrO_4$ [3]) and with other theoretical calculations (2.76 eV for $BaCrO_4$ [1]). Because of the decrease of the crystal symmetry from $BaCrO_4$ to $SrCrO_4$, the band gap of $SrCrO_4$ becomes narrower. For both $BaCrO_4$ and $SrCrO_4$, the difference between the lowest direct and indirect energy gaps is very small. Therefore a strong direct optical absorption is expected.

In general, GGA underestimates the energy band-gap as a result of self-interaction (a part of the exchange energy) problems. At an intermediate level between standards functional and more sophisticated many-body methods, methods such as DFT+U and hybrid DFT studies incorporate a U parameter or a fraction of the exact exchange in order to avoid the self-interaction problem partially and thus prevent the

band-gap underestimation. However, in this case, GGA (GGA+U with U=0) already overestimates the band-gap energy with respect to the experimental results. This also happens with other GGA theoretical results using different methodology and exchange-correlation functionals: 2.76 eV using the frozen-core all-electron projector augmented wave (PAW) method and plane wave-function basis sets [1]. Despite the GGA+U energy band gap overestimation, we will use several GGA+U schemes later for analyzing the more demanding optical properties, where in addition to the band energies, they will be needed to use the band occupations and transition probabilities (equation 1). It will make it possible to examine whether, in addition to the difference in the energy band gaps energies, there are large differences in the optical absorption.

The valence band (VB) edge of these compounds are made up mainly of $p(O_i)$ orbitals, whereas the conduction band (CB) edge is mainly made up of $d(Cr)$ orbitals. It is confirmed with a projected density of states (PDOS) on non-equivalent atomic species (Figure 2). In these structures the Cr atom is surrounded by $O_1+O_2+2O_3$ and $O_1+O_2+O_3+O_4$ atoms with approximately distorted tetrahedral symmetry in the Hashemite and Monazite structures respectively. Therefore, the $d(Cr)$ states split into d_e (d_{z^2} and $d_{x^2-y^2}$) and d_{t_2} (d_{xy} , d_{xz} , and d_{yz}) states whereas the s and p atomic states have a (s_a) and t_2 (p_t) tetrahedral symmetry respectively. The crystal wavefunctions with t_2 symmetry are mainly made up of the combination of the $d_{t_2}(Cr)$ and the states with t_2 symmetry of the neighboring $p_{t_2}(O_i)$ states. Therefore, the edge of the crystalline CB edge has t_2 symmetry.

In order to analyze the potential of these compounds as solar radiation absorbers, the absorption coefficients (AC) have been obtained (Figure 3). Despite the GGA+U energy band gap overestimation, the AC have been also obtained for different GGA+U schemes: U=0 eV (GGA), U=5 eV for the $d(Cr)$ states, and $U_{all}=5$ eV, where U=5 eV is

applied to the orbital subspace of all $d(\text{Cr})$, $p(\text{O})$ and $p(\text{B})$ ($\text{B}=\text{Ba}, \text{Sr}$) states. The DFT+U corrects the spurious self-interaction for the orbitals where the one-electron potential U is applied, while the remaining ones are still affected by the self-interaction error [9,10]. With $U=5$ eV [8,10] scheme we have only applied U to the d states of the transition metal atom as it is usual. Nevertheless, the effect on the band-gap when U is applied to an orbital group depends on the contribution from these orbitals to the band-gap edges [10]. If the contribution is small, the band-gap will remain almost unaffected. From the previous PDOS analysis the largest contribution to the VB edge is from $p(\text{O}_i)$ states, while that to the CB edge is from the $d(\text{Cr})$ states. This is the reason for using the $U_{\text{all}}=5$ eV scheme. The goal is to examine whether, in addition to the quantitative difference in the band gaps energies, there are large differences in the AC when GGA+U is used. These self-consistent calculations are more reasonable physically than applying a scissor operator or an artificial split in the bands ad hoc. For a better comparison, we shift the energy scale by the respective band gap energies. The main difference between the AC for the different U schemes is a shift resulting from the different energy band gap. The optical absorption peaks around 0.9 eV above the energy band gap (~ 3.60 eV and 3.55 eV for Hashemite- BaCrO_4 and Monazite- SrCrO_4 respectively with $U=0$ eV) compare well with the experimental absorbance peak of around 3.65 eV ($E-E_g \sim 1.0$ eV) from the results in the literature [3]. This peak is attributed to the electronic excitation from O to Cr states. The effect of relaxing all the atomic positions is also shown in Figure 3. This effect only slightly modifies the absorption coefficients. From the E_g energy gap to $E_g + 1.5$ eV approximately, the AC using GGA+U does not vary significantly with respect to GGA. The main differences are in the energy band gap. The optical absorption spectrum is consistent with that of a semiconductor with high absorption above the energy band gap.

With the purpose of identify [7,9,10] the different atomic and orbital contributions to the optical transitions, we split the AC into intra- and inter-non-equivalent species transitions. To do so, the $p_{\mu\lambda}$ momentum matrix element between the μ and λ bands is split in non-equivalent contributions such as $p_{\mu\lambda} = \sum_A \sum_B p_{\mu\lambda}^{AB}$. Here, $p_{\mu\lambda}^{AA}$ is the intra-species component that couples the localized basis set functions on the same atoms of the A non-equivalent species, whereas $p_{\mu\lambda}^{AB}$ (with $A \neq B$) is the inter-species component that couples the basis set functions on different atoms of the non-equivalent A and B species. The optical properties depend on the square of the momentum operator matrix elements. Therefore, they can be separated into three terms: intra-species (depending on $|p_{\mu\lambda}^{AA}|^2$), inter-species involving two non-equivalent A and B species of atoms (depending on $|p_{\mu\lambda}^{AB}|^2$), and inter-species involving three and four different non-equivalent A, B, C and D atoms (depending on $|p_{\mu\lambda}^{AB} || p_{\mu\lambda}^{CD}|$). The absorption coefficients and others optical properties can be split similarly.

The more interesting results, in which the AC is split into non-equivalent atomic species contributions, are shown in Figure 4. The largest contribution to the AC for lower energies corresponds to the Cr-O_i inter-species transitions, i.e. from $d_{12}(\text{Cr})$ to $p(\text{O}_i)$ states. The intra-species transitions between non-equivalent oxygen atoms (O_i-O_i) make a lower contribution than the Cr-O_i inter-atomic transitions. All other possibilities of inter- and intra-contributions not represented in the figure make a lower contribution than that represented. These results are in accordance with the previous PDOS analyses. These analyses are qualitative because only the band energies are considered. Nevertheless, with the AC splitting in Figure 4, the results are quantitative: band energies, momentum matrix elements and band populations have been considered (equation 1). Furthermore, from the results in Figure 4, the experimental absorbance

peak around 3.65 eV results in the literature [3] can be attributed to the Cr-O_i inter-species optical transitions from the $p(O_i)$ to $d_t(Cr)$ states.

Furthermore, we have developed a generalized multi-gap model to obtain maximum efficiencies in order to estimate the potentiality of these materials as multi-gap solar-cell devices. For multi-gap solar cells the presence of intermediate bands (IB) between the VB and the CB of the host semiconductor permits additional photon absorption and emission channels. The absorption of photons will be more efficient than in conventional solar cells because both VB-IB and IB-CB transitions are possible, allowing carrier generation from the VB to the CB. In addition to this carrier generation process, the usual process of generation through photon absorption promoting electrons from the VB to the CB also takes place. Therefore the current (electrons in CB and holes in VB) will be larger because of the sub-gap transitions and the efficiency of this device is larger than one based on the host semiconductor (conventional device with single-gap). The efficiency of a multi-gap solar cell can be obtained by using the ratio of the cell power output to the power cell density received [17,18]. The models used to obtain maximum efficiencies assume that any non-radiative recombination is suppressed, carrier mobilities are infinite (no ohmic losses), illumination comes from an isotropic gas of photons, and the cell absorbs all incident photons above the band-gap. For SrCrO₄ and BaCrO₄, with experimental band-gap energies 2.44 eV and 2.63 eV respectively [3], the limiting efficiencies are approximately between 60-74 % from double- to quintuple-gap solar cell. It are close to the absolute maximums of double-gap solar cell (60 % versus ~64 %) and of the large multiple-gap solar cell (74 % versus ~77 %) [17].

4. Conclusions

The electronic, structural and optical properties of $M\text{CrO}_4$ ($M=\text{Ba}, \text{Sr}$) have been analyzed using first principles. These analyses have been demanding because the difference between symmetrically non-equivalent atoms has been considered: five for the Hashemite- BaCrO_4 ($\text{BaCrO}_1\text{O}_2[\text{O}_3]_2$) and six for the Monazite- SrCrO_4 ($\text{SrCrO}_1\text{O}_2\text{O}_3\text{O}_4$). It implies, particularly for the optical properties, a greater number of projections and splits when the oxygen atoms are considered symmetrically non-equivalents. The results obtained agree well with the theoretical and experimental available data in the literature. The comparison between several U schemes shows that the main differences are in the quantitative energy band gap.

In order to relate the microscopic properties with the macroscopic optical properties, with direct relevance to use these materials as solar radiation absorbers, the latter have been split into inter- and intra-(symmetrically non-equivalent) species contributions. From these analyses, the absorption in these materials is mainly because of the Cr-O_i inter-species transitions, i.e. from the $d_{t_2}(\text{Cr})$ to $p(\text{O}_i)$ states. These results indicate that the effects of the M ($=\text{Ba}, \text{Sr}$) atoms on the optical properties are minimal in most cases. These properties are determined mainly by the CrO_4 tetrahedron. Therefore, a possible way to increase the optical absorption is develop new materials including the CrO_4 tetrahedron.

Acknowledgments

This work has been supported by the National Spanish projects PROMESA (ENE2012-37804-C02-01) and MADRID-PV (S2013/MAE-2780).

References

- [1] Xiao-Lin Wei, Li-Chun Xu, Yuan-Ping Chen, Li-Min Liu (2013) Structural and electronic properties of BaCrO₄ at high-pressures. *Solid State Communications* 155: 45–48.
- [2] Santamaría-Pérez D, Kumar R. S, Dos santos-García A. J, Errandonea D, Chuliá-Jordán R, Saez-Puche R, Rodríguez-Hernández P, and Muñoz A. (2012) High-pressure transition to the post-barite phase in BaCrO₄ hashemite. *Phys. Rev. B* 86: 094116.
- [3] Jiang Yin, Zhigang Zou, Jinhua Ye (2003) Photophysical and photocatalytic properties of new photocatalysts MCrO₄: (M=Sr, Ba). *Chemical Physics Letters* 378: 24–28.
- [4] Duesler E. N, Foord E. E. (1986) Crystal structure of Hashemite, BaCrO₄, a barite structure type. *American Mineralogist* 71: 1217-1220,.
- [5] Effenberger H. and Pertlik F. (1986) Four monazite type structures: comparison of SrCrO₄, SrSeO₄, PbCrO₄: (crocoite) and PbSeO₄. *Zeitschrift für Kristallographie* 176: 75 - 83.
- [6] Kohn W. and Sham L. J. (1965) Self-Consistent Equations Including Exchange and Correlation Effects. *Phys. Rev.* 140: A1133-A1138.
- [7] Private modification of the SIESTA code: Soler J. M, Artacho E, Gale J. D, García A, Junquera J, Ordejon P, and Sánchez-Portal D. (2002) The SIESTA Method for Ab initio Order-N Materials Simulation. *J. Phys.: Condens. Matter* 14: 2745-2779, and references therein.
- [8] Anisimov V. I, Zaanen J, and Andersen O. K. (1991) Band Theory and Mott Insulators: Hubbard U instead of Stoner I. *Phys. Rev. B* 44: 943-954; Anisimov V. I, Solovyev I. V. and Korotin M. A, Czyzyk M. T. and Sawatzky G. A. (1993) Density-Functional Theory and NiO Photoemission Spectra. *Phys. Rev. B* 48: 16929–16934.

- [9] Tablero C. (2008) Representations of the Occupation Number Matrix on the LDA/GGA+U Method. *J. Phys.: Condens. Matter* 20: 325205.
- [10] Tablero C. (2009) Effects of the Orbital Self-interaction in both Strongly and Weakly Correlated Systems. *J. Chem. Phys.* 130: 054903.
- [11] O'Regan D. D, Payne M. C. and Mostofi A. A. (2011) Subspace Representations in Ab initio Methods for Strongly Correlated Systems. *Phys. Rev. B* 83: 245124.
- [12] Grisolia M, Rozier P. and Benoit M. (2011) Density Functional Theory Investigations of the Structural and Electronic Properties of $\text{Ag}_2\text{V}_4\text{O}_{11}$. *Phys. Rev. B* 83: 165111.
- [13] Perdew J. P, Burke K. and Ernzerhof M. (1996) Generalized Gradient Approximation Made Simple. *Phys. Rev. Lett.* 77: 3865-3868.
- [14] Troullier N. and Martins J. L. (1991) Efficient Pseudopotentials for Plane-wave Calculations. *Phys. Rev. B* 43: 1993-2003.
- [15] Kleinman L. and Bylander D. M. (1982) Efficacious Form for Model Pseudopotentials. *Phys. Rev. Lett.* 48: 1425-1428; Bylander D. M. and Kleinman L. (1990) 4f Resonances with Norm-conserving Pseudopotentials. *Phys. Rev. B* 41: 907-912.
- [16] Sankey O. F. and Niklewski D. J. (1989) Ab initio Multicenter Tight-binding Model for Molecular-dynamics Simulations and Other Applications in Covalent Systems. *Phys. Rev. B* 40: 3979-3995.
- [17] Green M.A. (2003) Third Generation Photovoltaics. *Advanced Solar Energy Conversion*. Springer-Verlag Berlin Heidelberg, 2006.
- [18] A. Luque and A. Martí, Theoretical Limits of Photovoltaic Conversion, in *Handbook of Photovoltaic Science and Engineering* Edited by A. Luque and S. Hegedus, John Wiley & Sons Ltd (2003).

List of Figures

Figure 1: The (a) Hashemite-BaCrO₄ and (b) Monazite-SrCrO₄ crystal structures.

Figure 2: Projected density of states (per atom) on non-equivalent atoms and on the main shell atom states for the (a,c) Hashemite-BaCrO₄ and (b,d) Monazite-SrCrO₄ crystal structures. The VB edge has been chosen as the origin of the energy. The positive (negative) values correspond to the spin up (down) components.

Figure 3: Absorption coefficients $\alpha(E)$ for (a) Hashemite-BaCrO₄ and (b) Monazite-SrCrO₄ with $U_0/U_0(\text{rel})$ ($U=0$ eV without/with relaxing all atomic positions) and U_{all} ($U=5$ eV for d -Ba, d -Sr, d -Cr and p -O and orbitals). The respective band gap energies have been chosen as the origin of the energy.

Figure 4: More important intra- and inter-species absorption coefficients components with $U_0(\text{rel})$ for (a) Hashemite-BaCrO₄ and (b) Monazite-SrCrO₄. The energy scale has been shifted by the respective band gap energies.

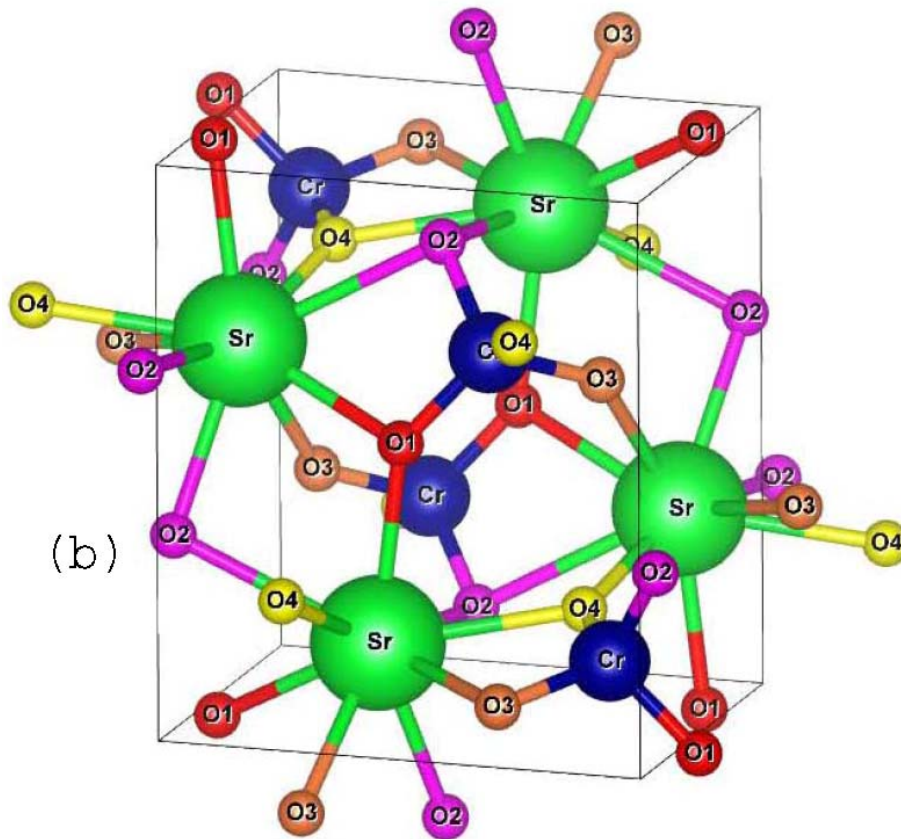
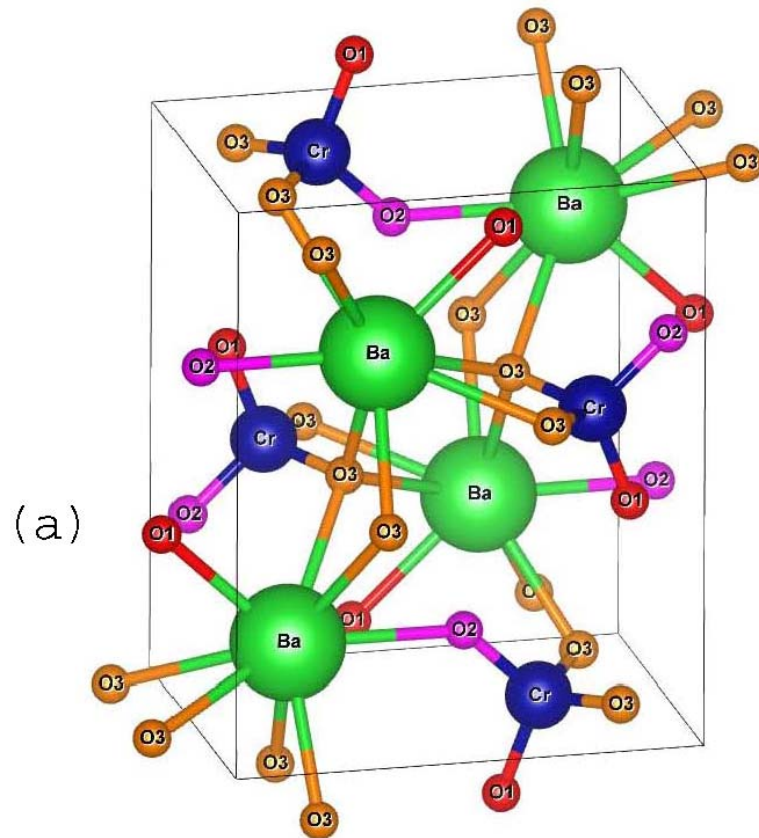


FIGURE 1

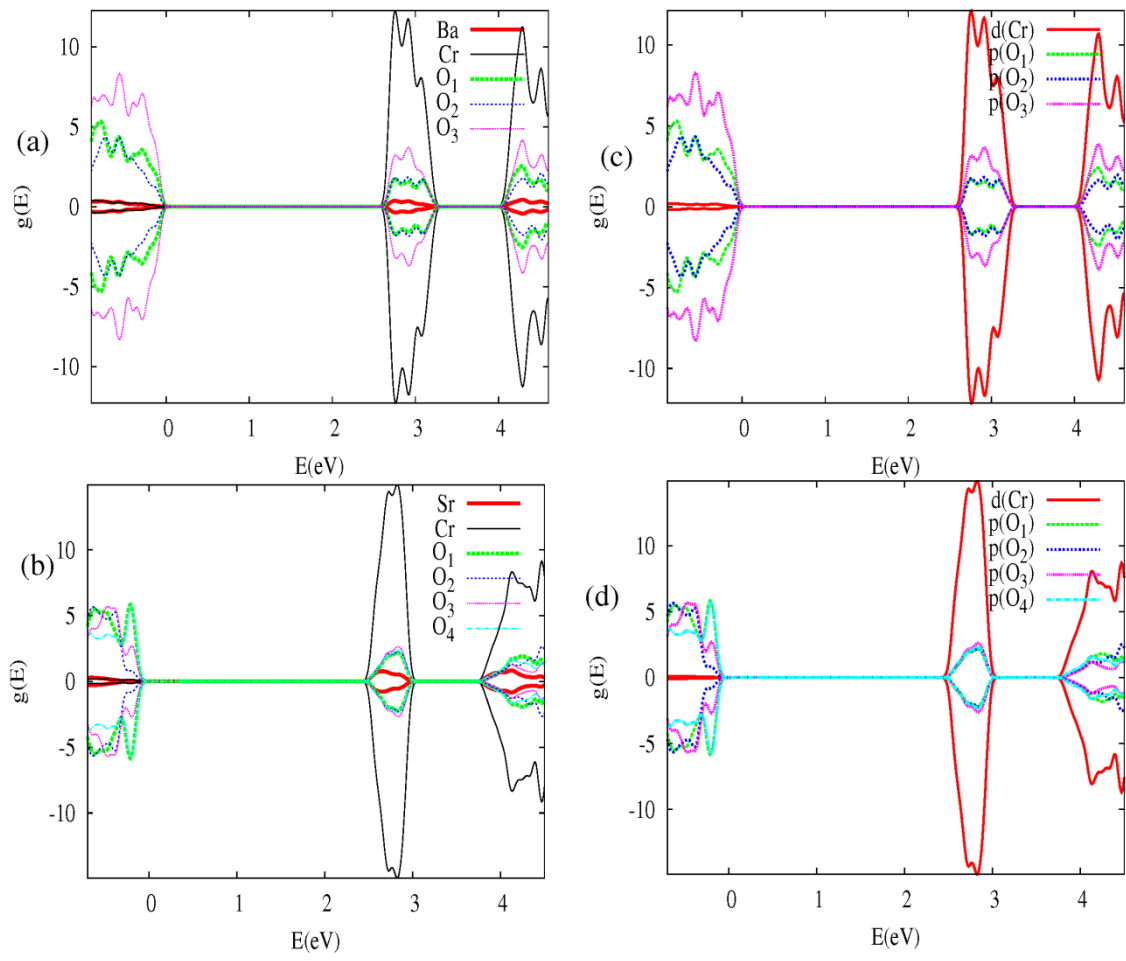


FIGURE 2

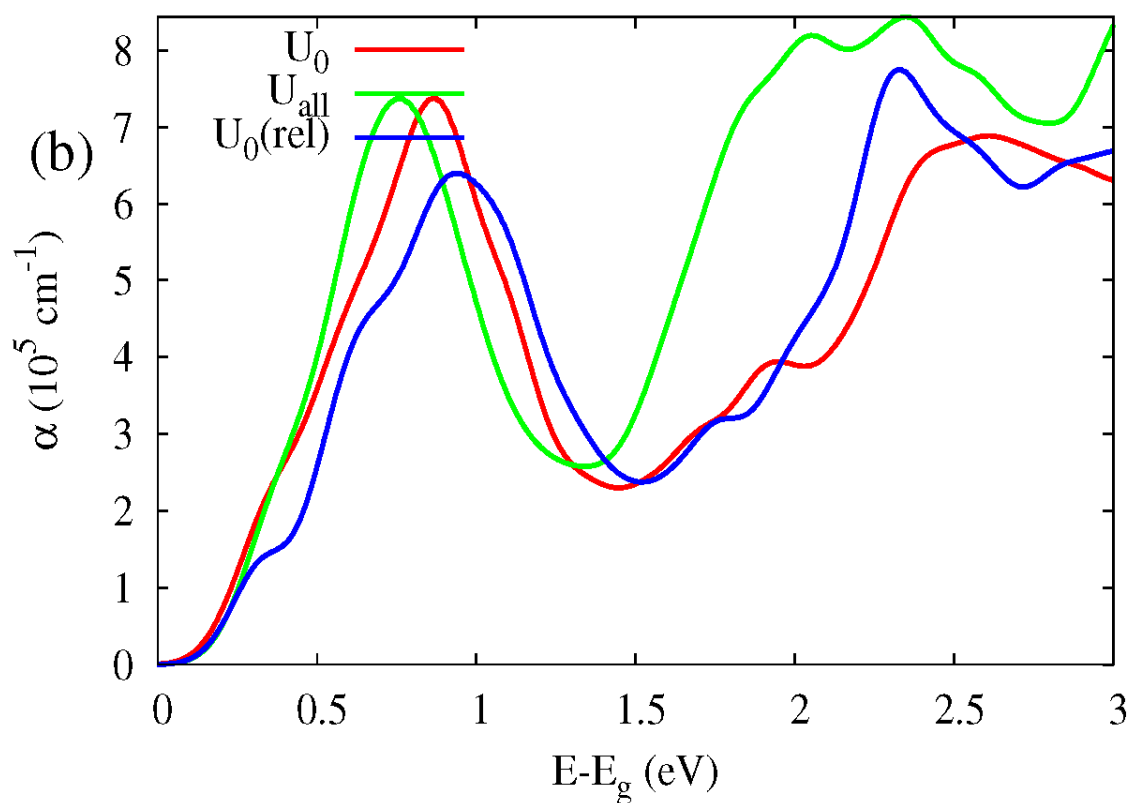
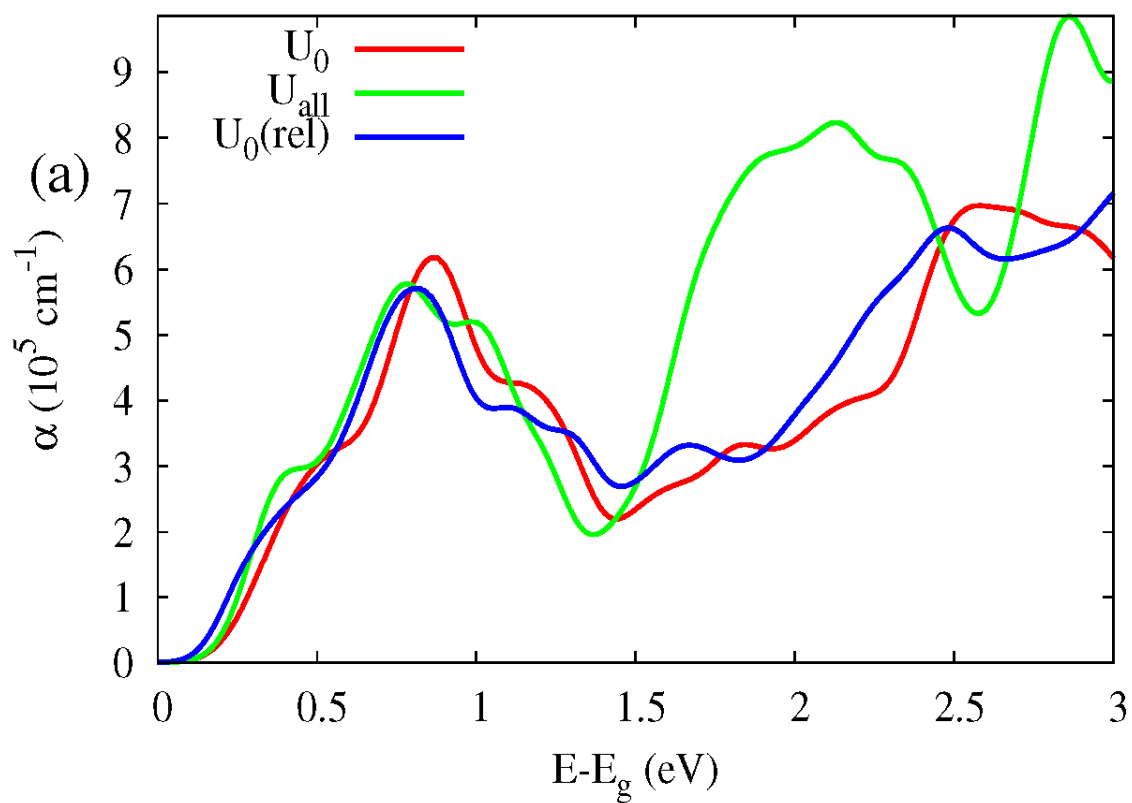


FIGURE 3

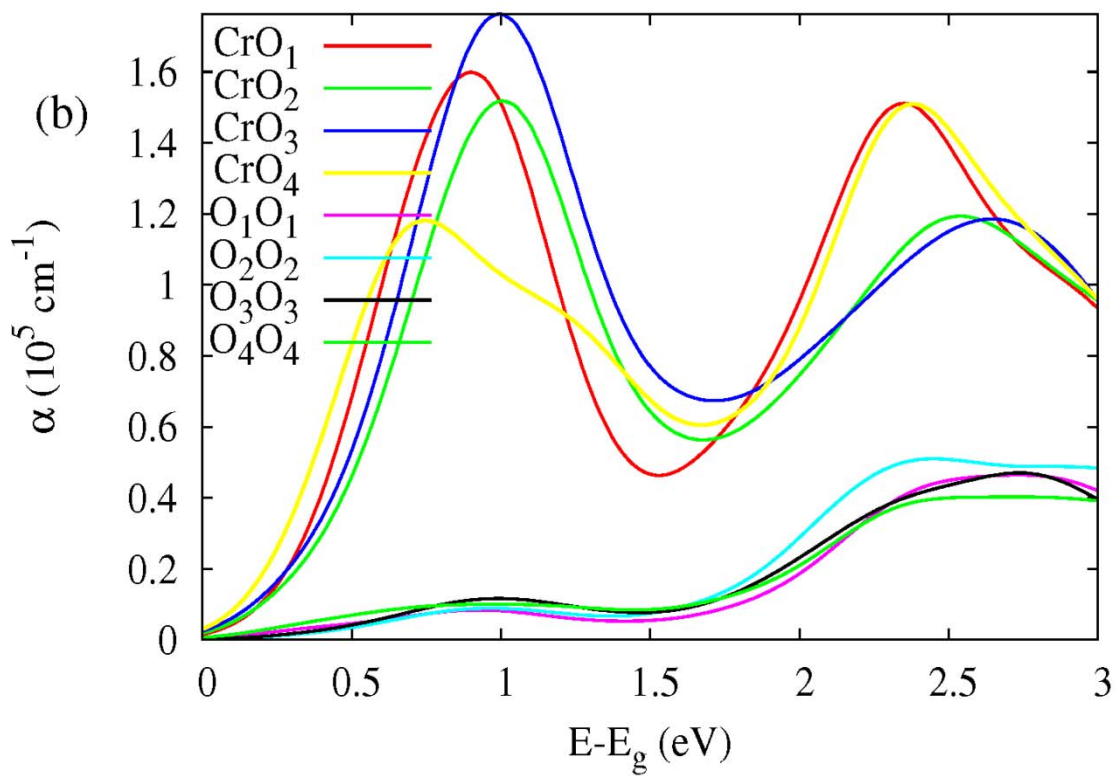
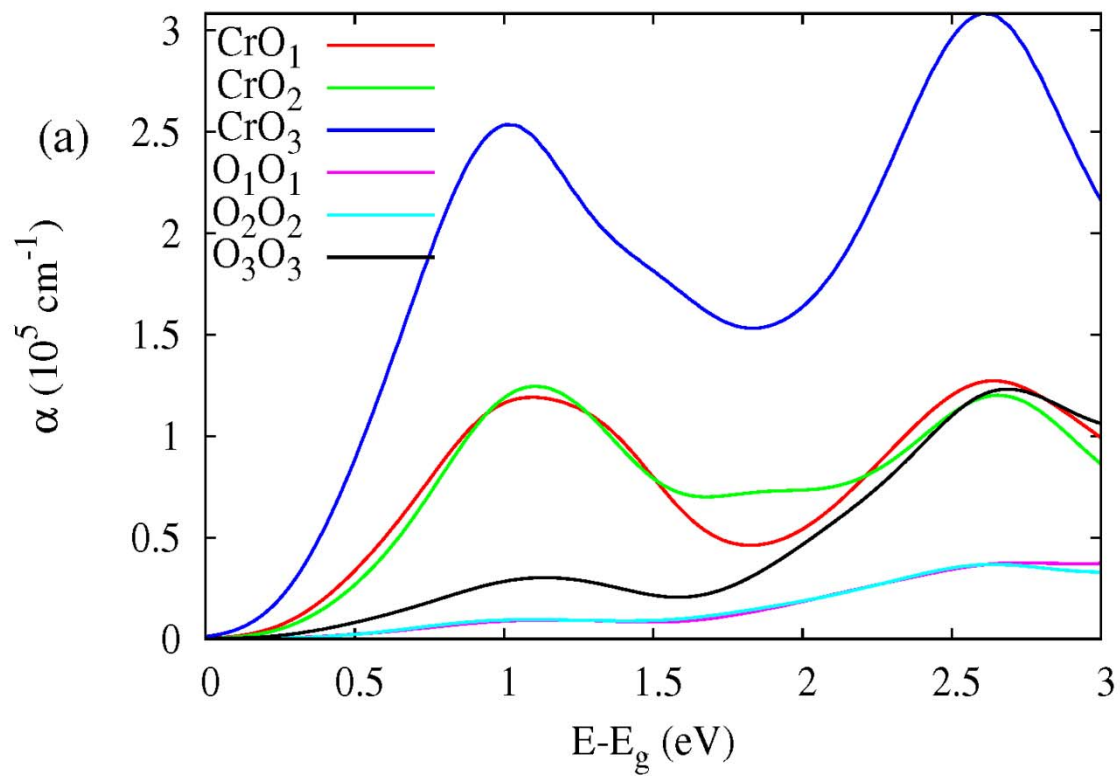


FIGURE 4